



**HAL**  
open science

# Association of Finite-Time Thermodynamics and a Bond-Graph Approach for Modeling an Endoreversible Heat Engine

Yuxiang Dong, Amin El-Bakkali, Georges Descombes, Michel Feidt, Christelle Périlhon

► **To cite this version:**

Yuxiang Dong, Amin El-Bakkali, Georges Descombes, Michel Feidt, Christelle Périlhon. Association of Finite-Time Thermodynamics and a Bond-Graph Approach for Modeling an Endoreversible Heat Engine. *Entropy*, 2012, 14 (4), pp.642–653. 10.3390/e14040642 . hal-01529404

**HAL Id: hal-01529404**

**<https://hal.science/hal-01529404>**

Submitted on 4 Sep 2023

**HAL** is a multi-disciplinary open access archive for the deposit and dissemination of scientific research documents, whether they are published or not. The documents may come from teaching and research institutions in France or abroad, or from public or private research centers.

L'archive ouverte pluridisciplinaire **HAL**, est destinée au dépôt et à la diffusion de documents scientifiques de niveau recherche, publiés ou non, émanant des établissements d'enseignement et de recherche français ou étrangers, des laboratoires publics ou privés.



Distributed under a Creative Commons Attribution 4.0 International License

Article

## Association of Finite-Time Thermodynamics and a Bond-Graph Approach for Modeling an Endoreversible Heat Engine

Yuxiang Dong <sup>1,2,\*</sup>, Amin El-Bakkali <sup>1</sup>, Georges Descombes <sup>2</sup>, Michel Feidt <sup>3</sup> and Christelle Périlhon <sup>2</sup>

<sup>1</sup> RENAULT, Advanced Electronics and Technologies Division, Technocentre Renault, 1 avenue de Golf 78288 Guyancourt, France; E-Mail: amin.el-bakkali@renault.com

<sup>2</sup> Laboratoire du génie des procédés pour l'environnement, l'énergie et la santé (LGP2ES-EA21), Cnam-Cemagref, case 2D3R20, 292 rue saint Martin 75003 Paris, France; E-Mails: georges.descombes@cnam.fr (G.D.); christelle.perilhon@cnam.fr (C.P.)

<sup>3</sup> Laboratoire d'Energétique et de Mécanique Théorique et Appliquée, ENSEM, 2, avenue de la Forêt de Haye 54516 Vandoeuvre, France; E-Mail: michel.feidt@ensem.inpl-nancy.fr

\* Author to whom correspondence should be addressed; E-Mail: yuxiang.dong@renault.com.

Received: 16 January 2012; in revised form: 13 March 2012 / Accepted: 23 March 2012 /

Published: 28 March 2012

---

**Abstract:** In recent decades, the approach known as Finite-Time Thermodynamics has provided a fruitful theoretical framework for the optimization of heat engines operating between a heat source (at temperature  $T_{hs}$ ) and a heat sink (at temperature  $T_{cs}$ ). The aim of this paper is to propose a more complete approach based on the association of Finite-Time Thermodynamics and the Bond-Graph approach for modeling endoreversible heat engines. This approach makes it possible for example to find in a simple way the characteristics of the optimal operating point at which the maximum mechanical power of the endoreversible heat engine is obtained with entropy flow rate as control variable. Furthermore it provides the analytical expressions of the optimal operating point of an irreversible heat engine where the energy conversion is accompanied by irreversibilities related to internal heat transfer and heat dissipation phenomena. This original approach, applied to an analysis of the performance of a thermoelectric generator, will be the object of a future publication.

**Keywords:** finite-time thermodynamics; bond graph approach; entropy generation; endoreversible heat engine; Chambadal-Novikov-Curzon-Ahlborn efficiency

---

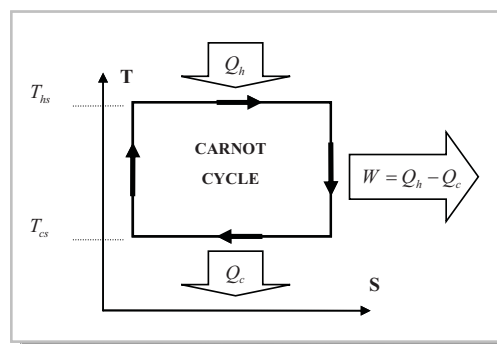
## Nomenclature

<i>Variable</i>	<i>Unit</i>	<i>Description</i>
$T_{hs}$	K	Temperature of the heat source
$T_{cs}$	K	Temperature of the heat sink
$T_h$	K	Hot side temperature of the endoreversible converter
$T_c$	K	Cold side temperature of the endoreversible converter
$\dot{S}_{hs}$	W/K	Entropy flow rate transferred from heat source to endoreversible converter
$\dot{S}_{cs}$	W/K	Entropy flow rate transferred from endoreversible converter to heat sink
$\dot{S}$	W/K	Entropy flow rate involved in energy converter
$\dot{S}_c$	W/K	Cutoff entropy flow rate
$\dot{\sigma}_T$	W/K	Rate of total entropy generation within the endoreversible heat engine
$K_h$	W/K	Global thermal conductance of the heat exchanger at hot side
$K_c$	W/K	Global thermal conductance of the heat exchanger at cold side
$\dot{Q}_h$	W	Thermal power exchanged between the heat source and the endoreversible converter
$\dot{Q}_c$	W	Thermal power exchanged between the heat sink and the endoreversible converter
$\dot{W}$	W	Mechanical power
$\dot{W}_{max}$	W	Maximum mechanical power
$\eta_l$	--	Energy conversion efficiency
$\eta_C$	--	Carnot efficiency
$\eta_{CNCA}$	--	Chambadal-Novikov-Curzon-Ahlaborn efficiency

## 1. Introduction

The energy conversion efficiency of a two-reservoir heat engine is generally compared with the theoretical efficiency of the Carnot engine. The Carnot engine assumes that the heat transfers at the heat source and at the heat sink occur without entropy production which excludes any thermal gradient (*cf.* Figure 1).

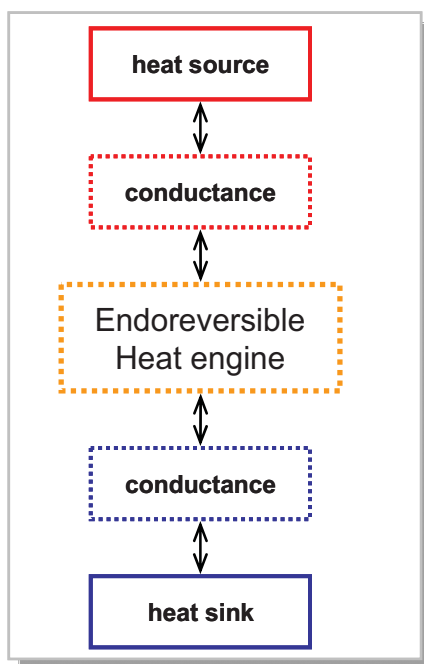
**Figure 1.** Carnot cycle in T-S diagram.



Without thermal gradients between the “working fluid” and the thermostats, the heat flow rate involved are zero which according to the first law of thermodynamics leads to the paradoxical fact that the Carnot heat engine produces zero mechanical power but with a maximum efficiency  $\eta_h = 1 - \frac{T_{cs}}{T_{hs}} = \eta_c!$

The question is whether there exists a more “realistic” limit of the energy conversion efficiency of bi-thermal heat engines besides the theoretical one of the Carnot engine. For this purpose, we have to admit that the heat exchange area and thus the global thermal conductances between the “working fluid” and the thermostats are finite. We then enter into the framework of a new approach of thermodynamics known as Finite-Time Thermodynamics, initiated independently by Chambadal [1] and Novikov [2] in 1957 and then clarified by Feidt [3] and others [4–8]. The main idea of this approach is the coupling of a reversible converter with two heat exchangers which connect the reversible converter to thermostats (*cf.* Figure 2). The heat exchangers are modeled by thermal conductances with finite values. The system then forms what we call an “Endoreversible Heat Engine” where only the irreversibilities related to external heat transfer between thermostats and the converter are taken into account. But in reality, for a real heat engine, in addition to irreversibilities seen previously, there are also internal irreversibilities within the converter (internal heat transfer, mechanical dissipation, *etc.*) [9]. Obtaining an analytical solution of such machines is very important for engineers seeking to optimize the design and the control of them. This will constitute the subject of our future paper.

**Figure 2.** Diagram of endoreversible heat engine.



Several studies have been conducted on this basis to optimize heat engines by taking finite constraints into account [10–15]. Besides the criterion of maximum conversion efficiency [16], other optimization criteria have been proposed: maximum power [17,18], maximum of power density [19], thermo-economic optimization [20,21] or ecological optimization [22,23].

Our approach detailed below is based on the association of the Finite-Time Thermodynamics approach and the Bond Graph Modeling approach [24]. The Bond-Graph Modeling approach

(*cf.* Figure 3) consists in expressing all the powers exchanged between two systems as the product of an effort variable  $e$  by a flow variable  $f$  (*cf.* Table 1). From a fundamental point of view, it is mainly based on the Onsager work [25,26]. In particular, a heat flow rate is the product of the temperature (effort variable) by the entropy flow rate (flow variable). The bond between two elements exchanging the power is completed by a half arrow indicating the positive direction of the power transfer (e.g., A to B, *cf.* Figure 3) and a so-called causal stroke indicating the element which imposes the effort on the other and receives the flow reaction.

**Figure 3.** Bond-Graph representation of power exchange between two physical systems.

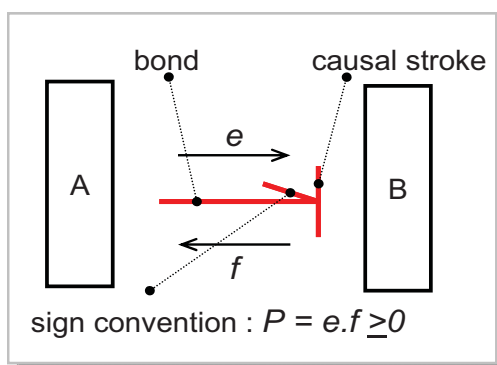


**Table 1.** Effort variables and flow variables in the multi-physical bond graph.

Power	Effort	Flow
Electrical	Voltage [V]	Current [A]
Mechanical, translation	Force [N]	Linear velocity [m/s]
Mechanical, rotation	Torque [N.m]	Angular velocity [rad/s]
Fluid	Pressure [N/m <sup>2</sup> ]	Volumetric flow rate [m <sup>3</sup> /s]
Thermal	Temperature [K]	Entropy flow rate [W/K]
Chemical	Chemical potential [J/mol]	molar flux [mol/s]

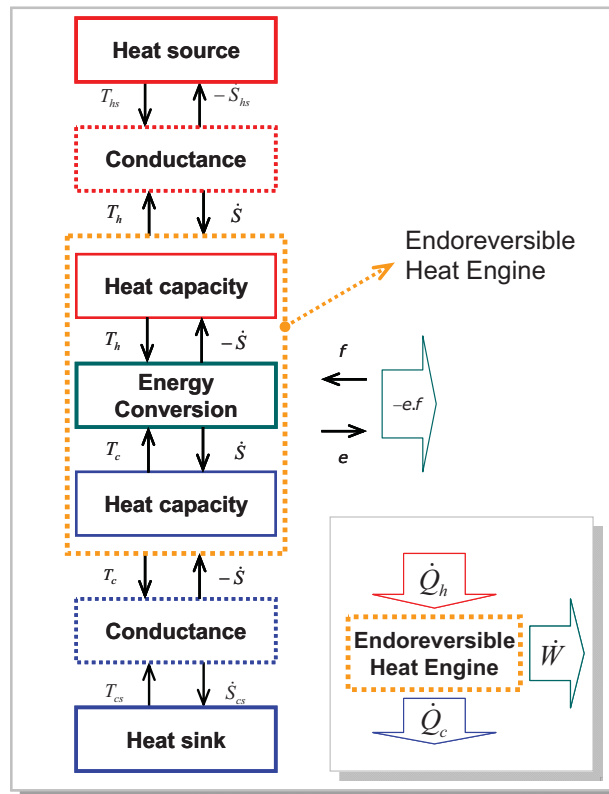
We will show in this paper that the combination of these two approaches allows one to find the natural control variable of the endoreversible heat engine and simplify the modeling of the system. In a subsequent paper we will give the analytical expressions of the characteristics of the optimal operating point of an irreversible heat engine, in which the energy conversion is accompanied by irreversibilities related to internal heat transfer and heat dissipation phenomena. By applying this new approach to a thermoelectric generator [27], the energy recovery potential can be expressed according to the physical parameters of the system.

The optimization criterion used here is based on the maximum mechanical power as it is a relevant criterion for heat recovery systems in which the heat source is considered “free” such as the exhaust gases of a motor vehicle. These heat recovery systems (ORC system, thermoelectric generator) are potentially interesting in view of the technical solutions designed to reduce the (Total Cost of Ownership) TCO of vehicles and greenhouse gas emissions.

## 2. Modeling of Endoreversible Heat Engine at Steady State

Figure 4 shows the Bond-Graph diagram of endoreversible heat engine. We assume that the machine works at steady state condition and thus, according to the second law of thermodynamics, we obtain the conservation of entropy flow rate  $\dot{S}$  through the reversible part of heat engine. By convention, the arrows next to the flow variables indicate the positive direction of power transfer.

**Figure 4.** Bond-Graph diagram of an endoreversible heat engine at steady state.



### 2.1. Energy Balance with Finite Heat Transfer Constraint

We make the following assumptions:

- The temperatures of heat source and heat sink are constant ( $T_{hs}$  and  $T_{cs}$ ).
- Heat exchangers have constant global thermal conductances ( $K_h$  and  $K_c$ ).
- The machine operates at steady state.

In this case, from the energy balances, we obtain:

$$\dot{Q}_h = \dot{S}_{hs} T_{hs} = \dot{S} T_h = K_h (T_{hs} - T_h) \tag{1}$$

$$\dot{Q}_c = \dot{S}_{cs} T_{cs} = \dot{S} T_c = K_c (T_c - T_{cs}) \tag{2}$$

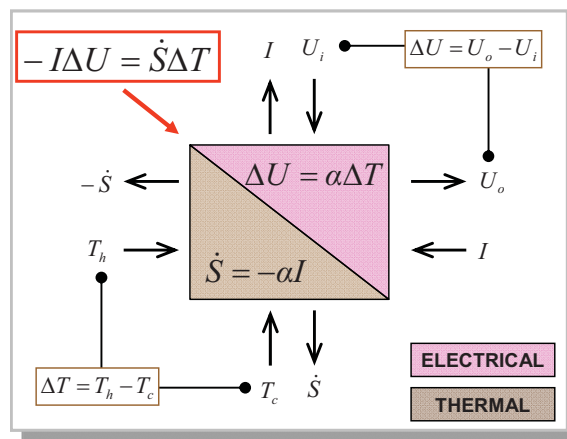
$$\dot{W} = -e.f = \dot{S}(T_h - T_c) = \dot{Q}_h - \dot{Q}_c \tag{3}$$

It can be seen that the mechanical power  $\dot{W} = \dot{S}(T_h - T_c)$  is expressed as the product of a current  $e$  (entropy flow rate) by a difference of potential  $f$  (temperatures). This is the advantage of the Bond-Graph representation which establishes analogies between different forms of energy.

2.2. Choice of the Control Variable of the Endoreversible Heat Engine

As shown in Figure 4, the endoreversible heat engine receives a flow  $f$  from the external environment and reacts with an effort  $e$  which depends on this flow, the conductances  $K_h, K_c$  and the temperatures  $T_{hs}$  and  $T_{cs}$  scale. Thus, the flow  $f$  represents the natural variable to control the endoreversible heat engine. In the case of thermoelectric conversion, the flow  $f$  represents the current imposed to the machine which reacts by the voltage (cf. Figure 5).

Figure 5. Diagram of thermoelectric conversion.



In this case, we have the relations  $\dot{S} = -\alpha \cdot f$  and  $e = \alpha(T_h - T_c)$  where  $\alpha$  is the Seebeck coefficient [27]. As a result, the entropy flow rate  $\dot{S}$  can act as control variable since it is the image of the flow variable  $f$ . This choice has the advantage of describing the operating point of the machine only by means of internal variables  $\dot{S}, T_h$  and  $T_c$ .

We can now, thanks to the relations (1) to (3), express the temperatures  $T_h$  and  $T_c$  then the thermal flux and the mechanical power as a function of the entropy flow rate  $\dot{S}$  inside the converter:

$$T_h = \frac{K_h T_{hs}}{K_h + \dot{S}}, T_c = \frac{K_c T_{cs}}{K_c - \dot{S}} \tag{4}$$

$$\dot{Q}_h = \dot{S} T_h = \frac{\dot{S} K_h T_{hs}}{K_h + \dot{S}}, \dot{Q}_c = \dot{S} T_c = \frac{\dot{S} K_c T_{cs}}{K_c - \dot{S}} \tag{5}$$

$$\dot{W} = \dot{S}(T_h - T_c) = \dot{S} \left( \frac{K_h T_{hs}}{K_h + \dot{S}} - \frac{K_c T_{cs}}{K_c - \dot{S}} \right) \tag{6}$$

The energy conversion efficiency can also be expressed in terms of entropy flow rate  $\dot{S}$  :

$$\eta_1 = \frac{\dot{W}}{\dot{Q}_h} = 1 - \frac{\dot{Q}_c}{\dot{Q}_h} = 1 - \frac{T_c}{T_h} = 1 - \frac{K_c T_{cs}}{K_h T_{hs}} \frac{K_h + \dot{S}}{K_c - \dot{S}} \tag{7}$$

When we vary the entropy flow rate  $\dot{S}$ , the operating point of the machine moves. The relations (6) and (7) then form the parametric equations of the operating curve of the endoreversible heat engine that we are going to study in the  $[\dot{W}, \eta_1]$  diagram.

2.3. Operating Range of the Endoreversible Heat Engine

The range of variation of the entropy flow rate  $\dot{S}$  for an endoreversible heat engine is implicitly defined by the inequality  $\dot{W}(\dot{S}) \geq 0$ . Note that the mechanical power  $\dot{W}(\dot{S})$  is zero at two remarkable points:

Point (A): zero entropy flow rate:	$\begin{aligned} \dot{S} &= 0 \\ T_h &= T_{hs}, T_c = T_{cs} \\ \dot{Q}_h &= \dot{Q}_c = 0 \\ \dot{W} &= 0, \eta_1 = 1 - \frac{T_{cs}}{T_{hs}} \end{aligned}$	(8)
Point (B): cutoff entropy flow rate:	$\begin{aligned} \dot{S} &= \dot{S}_{sc} = \frac{K_c K_h (T_{hs} - T_{cs})}{K_c T_{cs} + K_h T_{hs}} \\ T_h &= T_c = T_{sc} = \frac{K_c T_{cs} + K_h T_{hs}}{K_c + K_h} \\ \dot{Q}_h &= \dot{Q}_c = \dot{Q}_{sc} = \frac{K_c K_h (T_{hs} - T_{cs})}{K_c + K_h} = \dot{S}_{sc} T_{sc} \\ \dot{W} &= 0, \eta_1 = 0 \end{aligned}$	(9)

At point (A), the entropy flow rate is zero, the machine produces zero mechanical power but gives the maximum energy conversion efficiency, *i.e.*, Carnot efficiency. At point (B), with the cutoff entropy flow rate  $\dot{S}_{sc}$ , the machine behaves as two thermal resistances in series ( $1/K_c$  and  $1/K_h$ ) with the only effect that the thermal power  $\dot{Q}_{sc}$  is transferred from the heat source to the heat sink without any production of mechanical power. Finally, the parametric representation of the operating curve of the endoreversible heat engine (*cf.* Figure 6) in the  $[\dot{W}, \eta_1]$  diagram is given by the following relations:

$$0 \leq \dot{S} \leq \dot{S}_{sc}$$

$$\dot{W}(\dot{S}) = \dot{S} \left( \frac{K_h T_{hs}}{K_h + \dot{S}} - \frac{K_c T_{cs}}{K_c - \dot{S}} \right)$$

$$\eta_1(\dot{S}) = 1 - \frac{K_c T_{cs}}{K_h T_{hs}} \frac{K_h + \dot{S}}{K_c - \dot{S}}$$
(10)

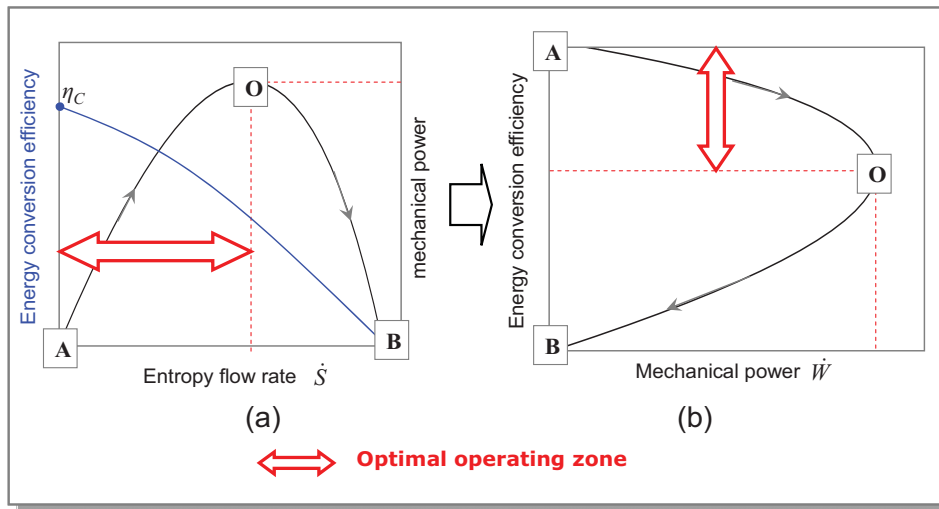
By deriving the mechanical power given by Equation (10) with regard to the entropy flow rate  $\dot{S}$  across the converter, we obtain:

$$\frac{d\dot{W}}{d\dot{S}} = \left( \frac{K_h \sqrt{T_{hs}}}{K_h + \dot{S}} \right)^2 - \left( \frac{K_c \sqrt{T_{cs}}}{K_c - \dot{S}} \right)^2, \quad \frac{d^2\dot{W}}{d\dot{S}^2} = -2 \left( \frac{K_h^2 T_{hs}}{(K_h + \dot{S})^3} + \frac{K_c^2 T_{cs}}{(K_c - \dot{S})^3} \right) \leq 0$$
(11)

Between points (A) and (B), there exists an optimal point (O) corresponding to the maximum mechanical power  $\dot{W}_{max}$ .



Figure 6. Operating curve of the endoreversible heat engine.



2.4. Determination of the Maximum Mechanical Power and the Associated Efficiency

The value of the entropy flow rate  $\dot{S}_o$  at the optimal point (O) can be obtained by solving the equation  $\frac{d\dot{W}}{d\dot{S}} = 0$  [cf. relation (11)]. Given the expressions (4) to (7), we obtain all the characteristics of the point (O):

Point (O): maximum mechanical power:

$$\left. \begin{aligned} \dot{S} = \dot{S}_o &= \frac{K_c K_h (\sqrt{T_{hs}} - \sqrt{T_{cs}})}{K_c \sqrt{T_{cs}} + K_h \sqrt{T_{hs}}} \\ \frac{T_{c,o}}{\sqrt{T_{cs}}} = \frac{T_{h,o}}{\sqrt{T_{hs}}} &= \frac{K_c \sqrt{T_{cs}} + K_h \sqrt{T_{hs}}}{K_c + K_h} \\ \frac{\dot{Q}_{c,o}}{\sqrt{T_{cs}}} = \frac{\dot{Q}_{h,o}}{\sqrt{T_{hs}}} &= \frac{K_c K_h (\sqrt{T_{hs}} - \sqrt{T_{cs}})}{K_c + K_h} \\ \dot{W}_{max} &= \frac{K_c K_h (\sqrt{T_{hs}} - \sqrt{T_{cs}})^2}{K_c + K_h} \\ \eta_1(\dot{W}_{max}) &= 1 - \sqrt{\frac{T_{cs}}{T_{hs}}} \end{aligned} \right\} \quad (12)$$

Finally, we obtain in a new way all the classical results and in particular the associated energy conversion efficiency at the optimal point  $\eta_{CNCA} = 1 - \sqrt{\frac{T_{cs}}{T_{hs}}}$  which depends only on the temperatures of heat source and heat sink [18].

The characteristics of this optimal point (O) can be determined through other ways. For example, Chambadal and Novikov chose the temperature  $T_h$  as control variable and through the energy and entropy balances, they obtained the mechanical power as function of the temperature  $T_h$  and then the optimal point is determined by a simple derivation [1,2]. The drawback of this method is that one can't directly control the temperature  $T_h$ . Other authors [18] used a more general method of Lagrange

multipliers to determine the optimal point but the inconvenient of this approach is that it doesn't give directly the characteristics of the operating curve of the machine.

The main advantage of our approach which consists of expressing all the variables of the heat engine as function of the entropy flow rate is that the operating range of the machine is explicitly defined by the cutoff entropy flow rate and this choice of control variable allows in a simple way to draw the operating curve of the machine and to determine the characteristics of the optimal point.

### 2.5. Analysis of the Rate of Entropy Generation

The expressions of the rate of entropy generation attached to heat transfers between the heat source/endoreversible converter and the endoreversible converter/heat sink can be obtained from simple entropy balance applied to the two conductances [cf. relation (5)]:

$$\dot{\sigma}_h = \dot{Q}_h \cdot \left( \frac{1}{T_h} - \frac{1}{T_{hs}} \right) \Rightarrow \dot{\sigma}_h = \frac{\dot{S}^2}{(K_h + \dot{S})} \geq 0 \tag{13}$$

$$\dot{\sigma}_c = \dot{Q}_c \cdot \left( \frac{1}{T_{cs}} - \frac{1}{T_c} \right) \Rightarrow \dot{\sigma}_c = \frac{\dot{S}^2}{(K_c - \dot{S})} \geq 0 \tag{14}$$

The rate of entropy generation can be written as the product of an extensive variable ( $\dot{Q}$ ) with the gradient of an intensive variable associated ( $\frac{1}{T}$ ). Each transformation is accompanied by certain entropy generation. In the absence of gradient of intensive variable (temperature, pressure, concentration, etc.), no transformation is possible (Onsager theory). The total rate of entropy generation in the case of an endoreversible heat engine becomes:

$$\dot{\sigma}_T = \dot{\sigma}_h + \dot{\sigma}_c = \frac{(K_c + K_h)\dot{S}^2}{(K_c - \dot{S})(K_h + \dot{S})} \geq 0 \tag{15}$$

By deriving twice the rate of total entropy generation  $\dot{\sigma}_T$  with regard to the entropy flow rate  $\dot{S}$ , we easily see that it increases faster and faster with the entropy flow rate (cf. Figure 7):

$$\frac{d\dot{\sigma}_T}{d\dot{S}} = \left[ \left( \frac{K_c}{K_c - \dot{S}} \right)^2 - \left( \frac{K_h}{K_h + \dot{S}} \right)^2 \right] \geq 0, \quad \frac{d^2\dot{\sigma}_T}{d\dot{S}^2} = 2 \left[ \frac{K_c^2}{(K_c - \dot{S})^3} + \frac{K_h^2}{(K_h + \dot{S})^3} \right] \geq 0 \tag{16}$$

In particular, at point (A) corresponding to zero entropy flow rate, the rate of entropy generation as well as its derivative are zero. By applying a second order Taylor expansion of the mechanical power and the rate of entropy generation around  $\dot{S} = 0$ , we obtain from Equations (11) and (16):

$$\dot{W}(\dot{S} \approx 0) \approx (T_{hs} - T_{cs})\dot{S}, \quad \dot{\sigma}_T(\dot{S} \approx 0) \approx \left( \frac{1}{K_c} + \frac{1}{K_h} \right) \dot{S}^2 \tag{17}$$

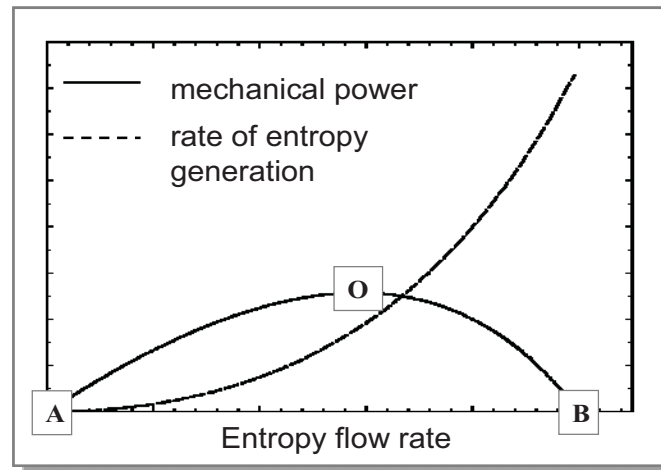
By eliminating the entropy flow rate  $\dot{S}$  between the two expressions (17), we obtain the relation:

$$\dot{\sigma}_T(\dot{W} \approx 0) \approx \left( \frac{1}{K_c} + \frac{1}{K_h} \right) \left( \frac{\dot{W}}{T_{hs} - T_{cs}} \right)^2 \tag{18}$$

which shows that in the neighborhood of the origin, the rate of entropy generation is of the second order with regard to the mechanical power produced. This result provides an explanation for the

paradoxical character of the Carnot engine which gives the best energy conversion efficiency with zero production of mechanical power!

**Figure 7.** Evolution of the mechanical power and the rate of entropy generation as a function of entropy flow rate.



### 3. Conclusions and Outlook

By associating Finite-Time Thermodynamics and the Bond-Graph approach, we have shown in this paper the interest of selecting the entropy flow rate  $\dot{S}$  involved in reversible energy conversion as the control variable of endoreversible heat engines. Indeed, this choice can be considered as a natural and convenient one to draw the operating curve of the machine. Furthermore, this choice allows one to obtain in a simple way:

- The expressions of all the variables as a function of the control variable.
- The range of variation of the control variable.
- The parametric equations of the operating curve of the machine.
- The characteristics of the optimal point according to the maximum mechanical power (CNCA efficiency,...). This approach is proposed in opposition to the great majority of existing results, using temperature as control variable (that is to say intensive variable and not extensive one).

In a second paper we will give the analytical expressions of the characteristics of the optimal operating point of an irreversible heat engine in which the energy conversion is accompanied by irreversibilities related to internal heat transfer and heat dissipation phenomena. By applying this proposed approach to a thermoelectric generator, the heat recovery potential can be estimated with regard to the physical parameters of thermoelectric cells and heat exchangers.

### References

1. Chambadal, P. *Les Centrales Nucléaires*; Armand Colin: Paris, France, 1957; pp. 41–58.
2. Novikov, I.I. The efficiency of atomic power station. *J. Nucl. Energy* **1958**, *7*, 125–128.
3. Feidt, M. *Thermodynamique et Optimisation Energétique des Systèmes et Procédés*; Lavoisier: Paris, France, 1987.

4. Jou, D.; Casas-Vasquez, J.; Lebon, G. *Extended Irreversible Thermodynamics*; Springer Verlag: Berlin, Germany, 2000.
5. Andresen, B. *Finite Time Thermodynamics*; Physics Laboratory, University of Copenhagen: Copenhagen, Denmark, 1983.
6. Bejan, A. Entropy generation minimization: The new thermodynamics of finite size, and finite time processes. *J. Appl. Phys.* **1997**, *79*, 1191–1218.
7. Bejan, A.; Tsatsaronis, G.; Moran, M. *Thermal Design and Optimization*; John Wiley & Sons: New York, NY, USA, 1996.
8. Goth, Y.; Feidt, M. Recherche sur les conditions optimales de fonctionnement des pompes à chaleur ou machines à froid associées à un cycle de Carnot endoreversible. *C. R. Acad. Sci.* **1986**, *303*, 113–122.
9. Chen, L.; Zhou, J.; Sun, F.; Wu, C. Ecological optimization for generalized irreversible Carnot engines. *Appl. Energy* **2004**, *77*, 327–338.
10. Chen, L.; Wu, C.; Sun, F. Finite time thermodynamic optimization or entropy generation minimization of energy systems. *J. Non-Equilib. Thermodyn.* **1999**, *24*, 327–359.
11. Chen, L.; Wu, C.; Sun, F.; Chen, W. Optimal performance of an endoreversible Carnot heat pump. *Energy Convers. Manag.* **1997**, *38*, 1439–1443.
12. Chen, L.; Wu, C.; Sun, F.; Chen, W. General performance characteristics of finite speed Carnot refrigerator. *Appl. Therm. Eng.* **1996**, *16*, 299–303.
13. Wu, C.; Kiang, R.L. Finite-time thermodynamic analysis of a Carnot engine with internal irreversibility. *Energy* **1992**, *17*, 1173–1178.
14. Feidt, M. Optimal thermodynamics—New upperbounds. *Entropy* **2009**, *11*, 529–547.
15. Feidt, M.; Costea, M.; Petre, C.; Petrescu, S. Optimization of the direct Carnot cycle. *Appl. Therm. Eng.* **2007**, *27*, 829–839.
16. Feidt, M. Reconsideration of criteria and modeling in order to optimize the efficiency of irreversible thermomechanical heat engines. *Entropy* **2010**, *12*, 2470–2484.
17. Curzon, F.L.; Ahlborn, B. Efficiency of a Carnot engine at maximum power conditions. *Am. J. Phys.* **1975**, *53*, 570–573.
18. Durmayaza, A.; Sogub, O.S.; Sahin, B.; Yavuz, H. Optimization of thermal systems based on finite-time thermodynamics and thermoeconomics. *Prog. Energy Combust. Sci.* **2004**, *30*, 175–217.
19. Kodal, A.; Sahin, B.; Yilmaz, T. A comparative performance analysis of irreversible Carnot heat engines under maximum power density and maximum power conditions. *Energy Convers. Manag.* **2000**, *41*, 235–248.
20. de Vos, A. Endoreversible thermoeconomics. *Energy Convers. Manag.* **1995**, *36*, 1–5.
21. Tyagi, S.K.; Chen, J.; Kaushik, S.C. Thermoeconomic optimization and parametric study of an irreversible Stirling heat pump cycle. *Int. J. Therm. Sci.* **2004**, *43*, 105–112.
22. Angulo-Brown, F. An ecological optimization criterion for finite-time heat engines. *J. Appl. Phys.* **1991**, *69*, 7465:1–7465:5.
23. Chen, L.; Zhou, J.; Sun, F.; Wu, C. Ecological optimization for generalized irreversible Carnot engines. *Appl. Energy* **2004**, *77*, 327–338.

24. Vijay, P.; Samantaray, A.K.; Mukherjee, A. A bond graph model-based evaluation of a control scheme to improve the dynamic performance of a solid oxide fuel cell. *Mechatronics* **2009**, *19*, 489–502.
25. Onsager, L. Reciprocal relations in irreversible processes. I. *Phys. Rev.* **1931**, *37*, 405–426.
26. Onsager, L. Reciprocal relations in irreversible processes. II. *Phys. Rev.* **1931**, *38*, 2265–2279.
27. Lenoir, B.; Michenaud, J.; Dauscher, A. Thermoélectricité: Des Principes aux Applications. *Technique de l'ingénieur* **2010**, Référence K730.

© 2012 by the authors; licensee MDPI, Basel, Switzerland. This article is an open access article distributed under the terms and conditions of the Creative Commons Attribution license (<http://creativecommons.org/licenses/by/3.0/>).